Int. J. Adv. Appl. Math. and Mech. 3(3) (2016) 79 – 91 (ISSN: 2347-2529)

Journal homepage: www.ijaamm.com

IJAAMM

International Journal of Advances in Applied Mathematics and Mechanics

Convective flow of nanofluid along a permeable stretching/shrinking wedge with second order slip using Buongiorno's mathematical model

Research Article

M. S. Alam[a,*], M. M. Haque[a], M. J. Uddin[b]

[a] *Department of Mathematics, Jagannath University, Dhaka-1100, Bangladesh*

[b] *Department of Mathematics and Statistics, College of Science, Sultan Qaboos University, P. O. Box 36, P. C. 123, Al-Khod, Muscat, Sultanate of Oman*

Received 19 October 2015; accepted (in revised version) 10 January 2016

Abstract: In this paper we have studied an unsteady two-dimensional laminar forced convective hydrodynamic heat and mass transfer flow of nanofluid along a permeable stretching/shrinking wedge with second order slip velocity using Buongiorno's mathematical model. Using appropriate similarity transformations, the governing non-linear partial differential equations are reduced to a set of non-linear ordinary differential equations which are then solved numerically using the function bvp4c from MATLAB for different values of the parameters. Numerical results for the non-dimensional velocity, temperature and nanoparticle volume fraction profiles as well as local skin-friction coefficient, local Nusselt number and local Sherwood number for different material parameters such as wedge angle parameter, unsteadiness parameter, Lewis number, suction parameter, Brownian motion parameter, thermophoresis parameter, slip parameter and Biot number are displayed in graphically as well as tabular form and discussed them from the physical point of view. The obtained numerical results clearly indicate that the flow field is influenced significantly by the second order slip parameter as well as surface convection parameter.

MSC: 76D05 • 65L60

Keywords: Nanofluid • Brownian motion • Stretching/Shrinking wedge • Second order slip flow

1. Introduction

Nanofluids refer to fluid suspensions of solid nano-sized particles in conventional heat transfer fluids, as Choi [1] first mentioned. Many types of liquids, such as water, ethylene glycol, engine oil, pump oil and glycerol have been used as host liquids in nanofluids. On the other hand, nanoparticles used in nanofluids have been made of various materials, such as oxide ceramics (Al_2O_3, CuO), nitride ceramics (AlN, SiN), carbide ceramics (SiC, TiC), metals (Cu, Ag, Au, Fe), semiconductors (TiO_2, SiC), etc. Since the thermal conductivity of the base fluids play important role on the heat transfer coefficient between the heat transfer medium and the heat transfer surface. Therefore, the effective thermal conductivity of nanofluids is expected to enhance heat transfer compared with conventional heat transfer liquids (Masuda et al. [2]). This phenomenon suggests the possibility of using nanofluids in advanced nuclear systems (Buongiorno and Hu [3]. These nanoparticles have unique chemical and physical properties (Oztop and Abu-Nada [4]) and have better thermal conductivity and convective heat transfer coefficient compared to the base fluid only. Choi et al. [5] showed that the addition of a small amount (less than 1% by volume) of nanoparticles to conventional heat transfer liquids increased the thermal conductivity of the fluid up to approximately two times.A comprehensive survey of convective transport in nanofluids was made by Buongiorno and Hu [3] and recently by Kakac and Pramuanjaroenkij [6]. We have also to mention the valuable recently published book by Das et al. [7] entitled Nanofluids: Science and Technology. Buongiorno and Hu [3] noticed that several authors have suggested that

* Corresponding author.

E-mail addresses: msalam631@yahoo.com (M. S. Alam), mojammelmath@gmail.com (M. M.Haque), jashim.fluidm@gmail.com (M. J. Uddin)

convective heat transfer enhancement could be due to the dispersion of the suspended nanoparticles but he argues that this effect is too small to explain the observed enhancement. He also concludes that turbulence is not affected by the presence of the nanoparticles so this cannot explain the observed enhancement. In another paper, Buongiorno [8] has pointed out that the nanoparticle absolute velocity can be viewed as the sum of the base fluid velocity and a relative velocity (that he calls the slip velocity). He considered in turn seven slip mechanisms: inertia, Brownian diffusion, thermophoresis, diffusiophoresis, Magnus effect, fluid drainage, and gravity settling. By comparing all the time scales of these processes he concluded that for laminar flow (also in the viscous sub-layer of the turbulent flow) thermophoresis and Brownian diffusion are important mechanisms, while in the turbulent region the nanoparticles are carried by turbulent eddies without slip and the diffusion mechanisms above are negligible there. Based on these assumptions, he also derived the continuity equation for nanofluids and nanoparticle volume fraction. The steady boundary-layer flow of a nanofluid past a moving semi-infinite flat plate in a uniform free stream has been investigated by Bachok et al. [9]. Recently Khan and Pop [10] studied the problem of steady boundary layer flow past a wedge moving in nanofluid. Very recently, Rajput et al. [11] studied the boundary layer flow of an electrically conducting, viscous incompressible nanofluids over moving surface in the presence of uniform magnetic field.

Therefore the objective of the present study is to investigate the effects of thermophoresis and Brownian motion on an unsteady two-dimensional forced convective flow of nanofluid along a permeable stretching/shrinking wedge in the presence of variable suction and second order slip.

2. Physical model and mathematical formulation

Let us consider an unsteady two-dimensional laminar forced convective heat and mass transfer flow of a water based nanofluid along a permeable stretching/shrinking wedge. The angle of the wedge is given by $\Omega = \beta\pi$ as shown in Fig. 1. The flow is assumed to be in the x -direction which is taken along the direction of the wedge and the y-axis normal to it. It is assumed that the lower surface of the wedge is heated by convection from a hot fluid of temperature, T_f which provides a heat transfer coefficient h_f. Fluid suction is considered along the wedge surface. The physical model and co-ordinate system are shown in Fig. 1

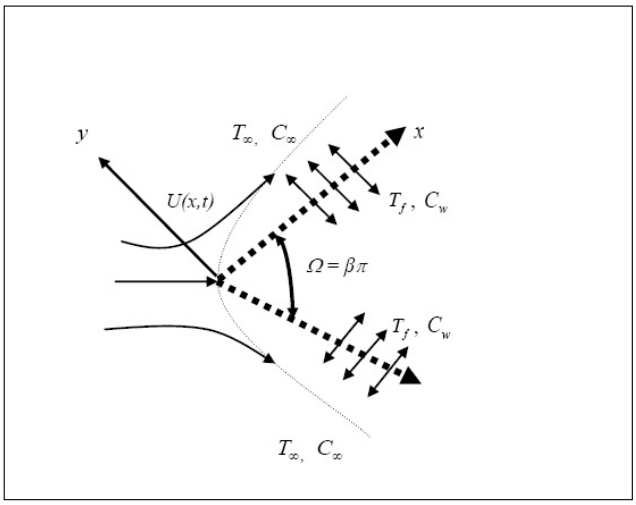

Fig. 1. Flow configuration and co-ordinate system.

We will treat the nanofluid as a two component mixture (base fluid + nanoparticles) with the following assumptions (see also Buongiorno [8]):
(i) incompressible flow, (ii) no chemical reactions, (iii) negligible external forces, (iv) dilute mixture ($\phi \ll 1$), (v) negligible viscous dissipation, (vi) negligible radiative heat transfer, (vii) nanoparticles and base fluid locally in thermal equilibrium.
Then under the above assumptions and boundary-layer approximation, the governing equations describing the conservation of mass, momentum, energy and nanoparticle volume fraction, respectively can be written as follows (see also Khan and Pop [10] for steady case):

$$\frac{\partial u}{\partial x} + \frac{\partial v}{\partial y} = 0 \tag{1}$$

$$\frac{\partial u}{\partial t} + u\frac{\partial u}{\partial x} + v\frac{\partial u}{\partial y} = \frac{\partial U}{\partial t} + U\frac{\partial U}{\partial x} + \nu\frac{\partial^2 u}{\partial y^2} \tag{2}$$

$$\frac{\partial T}{\partial t}+u\frac{\partial T}{\partial x}+v\frac{\partial T}{\partial y}=\alpha\frac{\partial^2 T}{\partial y^2}+\tau\left[D_B\frac{\partial C}{\partial y}\frac{\partial T}{\partial y}+\left(\frac{D_T}{T_\infty}\right)\left(\frac{\partial T}{\partial y}\right)^2\right] \tag{3}$$

$$\frac{\partial C}{\partial t}+u\frac{\partial C}{\partial x}+v\frac{\partial C}{\partial y}=D_B\frac{\partial^2 C}{\partial y^2}+\left(\frac{D_T}{D_B}\right)\left(\frac{\partial^2 T}{\partial y^2}\right) \tag{4}$$

where u, v are the velocity components along the axes x and y respectively, t is the time, α is the thermal diffusivity of the base fluid, ν is the kinematic viscosity, D_B is the Brownian diffusion coefficient, D_T is the thermophoretic diffusion coefficient, $\tau=\dfrac{(\rho c)_p}{(\rho c)_f}$ is the ratio between the effective heat capacity of the nanoparticles material and heat capacity of the fluid, T is the temperature of the nanofluid inside the boundary layer, T_∞ is the temperature of the ambient fluid outside the boundary layer, C is the nanoparticles volume fraction while C_∞ is its ambient value.

3. Boundary conditions

The boundary conditions for the above stated model are as follows:

$$u=\lambda U+A\frac{\partial u}{\partial y}+B\frac{\partial^2 u}{\partial y^2}\qquad v=v_w(x,t),\quad -\kappa\frac{\partial T}{\partial y}=h_f(T_f-T)\quad C=C_w\quad at\quad y=0 \tag{5}$$

$$u=U(x,t)\qquad T\to T_\infty,\qquad C\to C_\infty\qquad as\qquad y\to\infty \tag{6}$$

where A and B are the first and second order slip constants respectively (see Fang et al. [13]), $v_w(x,t)$ is the suction velocity at the wall, and $U(x,t)$ is the potential velocity generated by the pressure gradient. Here λ is a constant so that $\lambda>0$ corresponds to a stretching wedge and $\lambda<0$ for a shrinking wedge while $\lambda=0$ for a static wedge.
Following Sattar [12], the potential flow velocity for the wedge flow is taken as:

$$U(x,t)=\frac{\nu x^m}{\delta^{m+1}} \tag{7}$$

where m is an arbitrary constant and is related to the wedge angle and δ is the time-dependent length scale which is taken to be (see also Sattar [12], Alam and Huda [14] and Alam et al. [15]) as:

$$\delta=\delta(t) \tag{8}$$

4. Non-dimensionalization

In order to obtain the local similarity solutions of the governing equations (1)-(4) together with the boundary conditions (5) and (6) we introduce the following non-dimensional variables (see also Rahman et. al. [16]):

$$\eta=y\sqrt{\frac{m+1}{2}}\sqrt{\frac{x^{m-1}}{\delta^{m+1}}},\quad \psi=\sqrt{\frac{2}{m+1}}\frac{\nu x^{(m+1)/2}}{\delta^{(m+1)/2}}f(\eta),\quad \theta(\eta)=\frac{T-T_\infty}{T_f-T_\infty},\quad \phi(\eta)=\frac{C-C_\infty}{C_w-C_\infty} \tag{9}$$

where η is the similarity variable, ψ is the stream function that satisfies the continuity equation (1) and is defined by $u=\dfrac{\partial\psi}{\partial y}$ and $v=-\dfrac{\partial\psi}{\partial x}$. Since $u=\dfrac{\partial\psi}{\partial y}$ and $v=-\dfrac{\partial\psi}{\partial x}$, we have from equation (9)

$$u=U(x,t)f' \tag{10}$$

and

$$v=-\sqrt{\frac{2}{m+1}}\frac{(m+1)}{2}\frac{\nu x^{(m-1)/2}}{\delta^{(m+1)/2}}\left(f+\frac{m-1}{m+1}\eta f'\right) \tag{11}$$

Now using equations (7)-(11) into equations (2)-(4) we obtain the following non-linear ordinary differential equations:

$$f'''+f''f+\beta(1-f'^2)-K(2-2f'-\eta f'')=0 \tag{12}$$

$$\theta'' + Pr f\theta' + PrNb\theta'\phi' + PrNt\theta'^2 + PrK\eta\theta' = 0 \tag{13}$$

$$\phi'' + Lef\phi' + \frac{Nt}{Nb}\theta'' + LeK\eta\phi' = 0 \tag{14}$$

subject to the transformed boundary conditions:

$$f = F_w, \quad f' = \lambda + af'' + bf''', \quad \theta' = Bi(\theta - 1) \quad \phi = 1 \quad at \quad \eta = 0 \tag{15}$$

$$f' = 1, \quad \theta = 0 \quad \phi = 0 \quad as \quad \eta \to \infty \tag{16}$$

Here, prime(s) denote differentiation with respect to the similarity variable η, $F_w = -\dfrac{v_w(x,t)}{\left(\sqrt{\frac{(m+1)}{2}}\frac{\nu x^{\frac{m-1}{2}}}{\delta^{\frac{m+1}{2}}}\right)}$ represents the wall mass transfer coefficient which is positive for suction and negative for injection but for the present problem we have consider only suction velocity and λ is the stretching/shrinking parameter according as positive/negative respectively.

5. Important physical parameters

The dimensionless parameters which appear in the equations (12)-(15) are defined as follows: $\beta = \dfrac{2m}{m+1}$ is the wedge angle parameter that corresponds to $\Omega = \beta\pi$ for a total angle Ω of the wedge, $K = \dfrac{\delta^m}{\nu x^{m-1}}\dfrac{d\delta}{dt}$ is the unsteadiness parameter, $Pr = \dfrac{\nu}{\alpha}$ is the Prandtl number for the base fluid, $Nb = \dfrac{\tau D_B(C_w - C_\infty)}{\nu}$ is the Brownian motion parameter, $Nt = \dfrac{\tau D_B(T_f - T_\infty)}{\nu T_\infty}$ is the thermophoresis parameter and $Le = \dfrac{\nu}{D_B}$ is the Lewis number, $a = A\sqrt{\dfrac{m+1}{2}}\sqrt{\dfrac{x^{m-1}}{\delta^{m+1}}}$ is the first order velocity slip parameter, $b = B\dfrac{m+1}{2}\dfrac{x^{m-1}}{\delta^{m+1}}$ is the second order velocity slip parameter and $Bi = \sqrt{\dfrac{2}{m+1}}Re_x^{-\frac{1}{2}}\dfrac{h_f x}{\kappa}$ is the Biot number or surface convection parameter.
We notice that when F_w, Nb and Nt are zero, then equations (12) and (13) involve just two dependent variables, namely, $f(\eta)$ and $\theta(\eta)$, and the boundary-value problem for these two variables reduces to the classical problem for an impermeable moving surface in a Newtonian fluid. The boundary-value problem for $\phi(\eta)$ then becomes ill-posed and is of no physical significance. It is also important to note that this boundary-value problem reduces to the classical Falkner-Skan's problem of the boundary layer flow of a viscous and incompressible fluid past a fixed wedge, when β and K are zero in equation (12).

6. Parameters of engineering interest

The parameters of engineering interest in the present problem are the local skin friction coefficient Cf_x, the local Nusselt number Nu_x and the local Sherwood number Sh_x , which are obtained from the following relations:

$$Cf_x Re_x^{1/2} = \frac{2}{\sqrt{2-\beta}} f''(0) \tag{17}$$

$$Nu_x Re_x^{-1/2} = -\frac{1}{\sqrt{2-\beta}}\theta'(0) \tag{18}$$

$$Sh_x Re_x^{-1/2} = -\frac{1}{\sqrt{2-\beta}}\phi'(0) \tag{19}$$

where $Re = \dfrac{Ux}{\nu}$ is the local Reynold's number.

7. Numerical solutions

The system of ordinary differential equations (12)-(14) are highly nonlinear and therefore the system cannot be solved analytically. Following Rahman et al. [17]-[19], the system of transformed governing nonlinear ordinary differential equations (12)-(14) together with the boundary conditions (15)-(16) are locally similar and are solved numerically by using the function bvp4c from MATLAB for different values of the parameters. Examples of solving boundary value problems by bvp4c can be found in the book by Shampine et al. [20] or through online tutorial by Shampine et al. [21]. The numerical simulations are carried out for various values of the physical parameters such as wedge angle parameter (β), unsteadiness parameter (K), Lewis number (Le), Brownian motion parameter (Nb), thermophoresis parameter (Nt), suction parameter (F_W), stretching/shrinking parameter (λ), first order slip parameter (a), second order slip parameter (b) and Biot number (Bi). Because of the lack of experimental data, the choice of the values of the parameters was dictated by the values chosen by previous investigators. The values of the Prandtl number, Lewis number, Brownian motion parameter and thermophoresis parameter are set equal to 6.8, 10, 0.2, and 0.2, respectively, throughout the paper unless otherwise specified. The code bvp4c is developed using finite element method. The mesh selection and error control are based on the residual of the continuous solution. The relative error tolerance has been set to 10^{-6}.

7.1. Code verification and comparison with previous work

To check the validity of the present code, we have calculated the values of $f(\eta)$, $f'(\eta)$ and $f''(\eta)$ for the Falkner-Skan boundary layer equation for the case $\beta = 0$, $F_w = 0$ (impermeable wedge) and $K = 0$ (for steady flow) for different values of η . Thus from Table 1, we observe that the data produced by the present code and those of White [22] are in excellent agreement which gives us confidence to use the present numerical code.

Table 1. Comparison of the present numerical results of Falkner-Skan boundary layer equation for the case of $\beta = K = F_w = 0$ and $Pr = 0.71$.

η	$f(\eta)$		$f'(\eta)$		$f''(\eta)$	
	present work	White[22]	present work	White[22]	present work	White[22]
0.0	0.0000000	0.00000	0.00000000	0.00000	0.46964218	0.46960
0.5	0.05865082	0.05864	0.23424831	0.23423	0.46507107	0.46503
1.0	0.23301626	0.23299	0.46067192	0.46063	0.43441274	0.43438
1.5	0.51508336	0.51503	0.66152592	0.66147	0.36182459	0.36180
2.0	0.88687819	0.88680	0.81675164	0.81669	0.25567446	0.25567
3.0	1.79570660	1.79557	0.96910685	0.96905	0.06770503	0.06771
4.0	2.78407530	2.78388	0.99781828	0.99777	0.00687281	0.00687
5.0	3.78347123	3.78323	0.99998350	0.99994	0.00025771	0.00026

8. Results and discussion

Numerical solutions have been carried out for different values of parameters such as wedge angle parameter (β), unsteadiness parameter (K) , Lewis number (Le) , suction parameter (F_w), Brownian motion parameter (Nb), thermophoresis parameter (Nt), stretching/shrinking parameter (λ), first order slip parameter (a), second order slip parameter (b) and Biot number (Bi) on the flow, heat and mass transfer characteristics. In the numerical simulation, we have considered water-based nanofluids (containing Cu, Al_2O_3, TiO_3, etc. nanoparticles). The value of Prandtl number for the base fluid is kept as $Pr = 6.8$ (at the room temperature). The default values of the other parameters are taken as $\beta = 0.2$, $K = 0.2$, $Le = 10.0$, $F_w = 0.5$, $Nb = 0.2$, $Nt = 0.2$, $\lambda = 1.0$, $a = 0.5$, $b = -0.2$, and $Bi = 1.0$ unless otherwise specified.

The effects of the stretching parameter $\lambda > 0$ on the non-dimensional velocity, temperature and nanoparticle volume fraction profiles within the boundary layer is shown in Fig. 2(a)-(c) respectively. From these figures we observe that the velocity profiles decrease whereas both the temperature of the fluid and nanoparticle volume fraction profiles within the boundary layer decrease with the increasing values of the stretching parameter (λ).

Fig. 3(a)-(c) respectively show the non-dimensional velocity, temperature and nanoparticle volume fraction profiles within the boundary layer for different values of the shrinking parameter $\lambda < 0$. The behavior of these figures are just opposite to the Fig. 2(a)-(c) respectively.

The effect of changes in the wedge angle parameter β on the dimensionless velocity function f' against η is displayed in Fig. 4(a) for the values 0.0, 0.5, 1.0 and 1.8. The value $\beta = 0$ corresponds to wedge angle of zero degree i.e. flat plate and $\beta = 0.5$ corresponds to the wedge angle of 90 degrees i.e. the vertical plate. From this figure it is clear

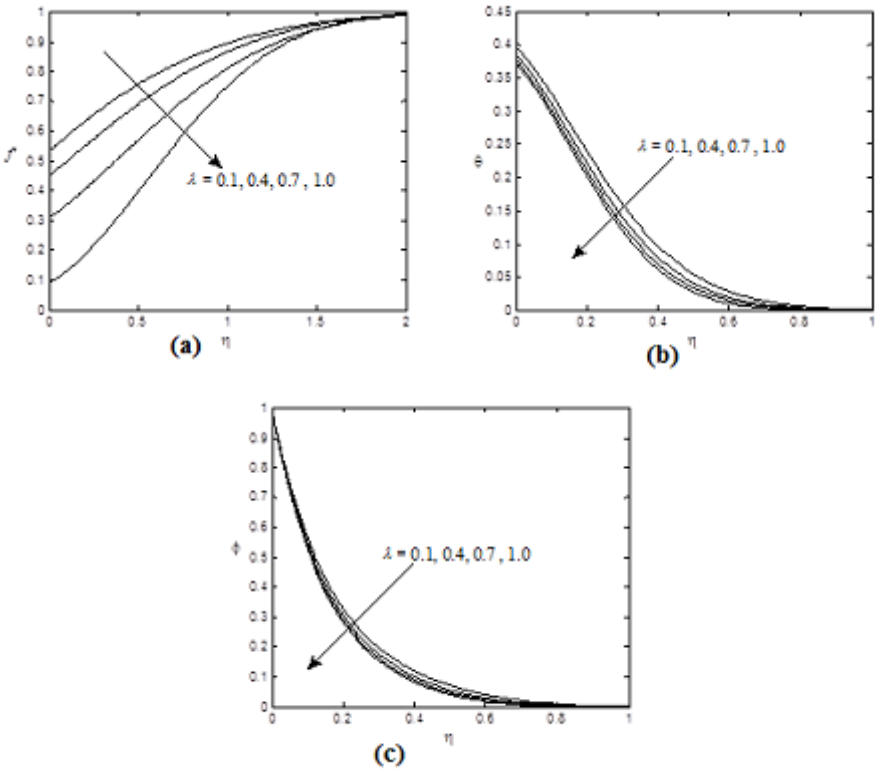

Fig. 2. Variation of dimensionless (a) velocity, (b) temperature and (c) nanoparticle volume fraction profiles for several values of stretching parameter λ.

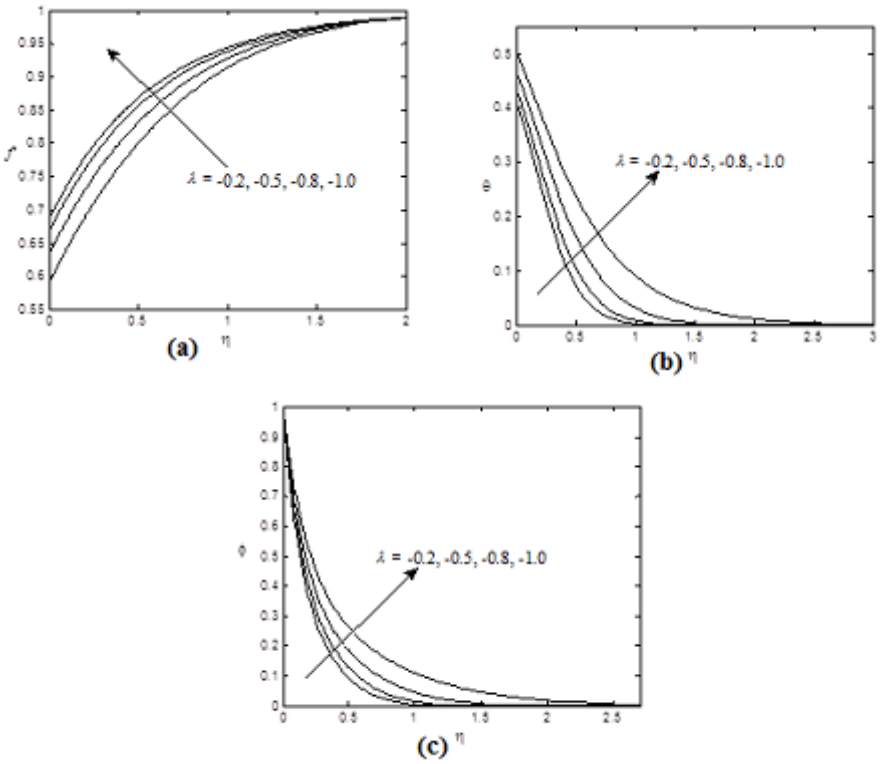

Fig. 3. Variation of dimensionless (a) velocity, (b) temperature and (c) nanoparticle volume fraction profiles for several values of shrinking parameter λ.

that as the wedge angle parameter β increases the fluid velocity within the boundary layer also increases. On the other hand from Fig. 4(b)-(c) we see that both the non-dimensional temperature and nanoparticle volume fraction profiles

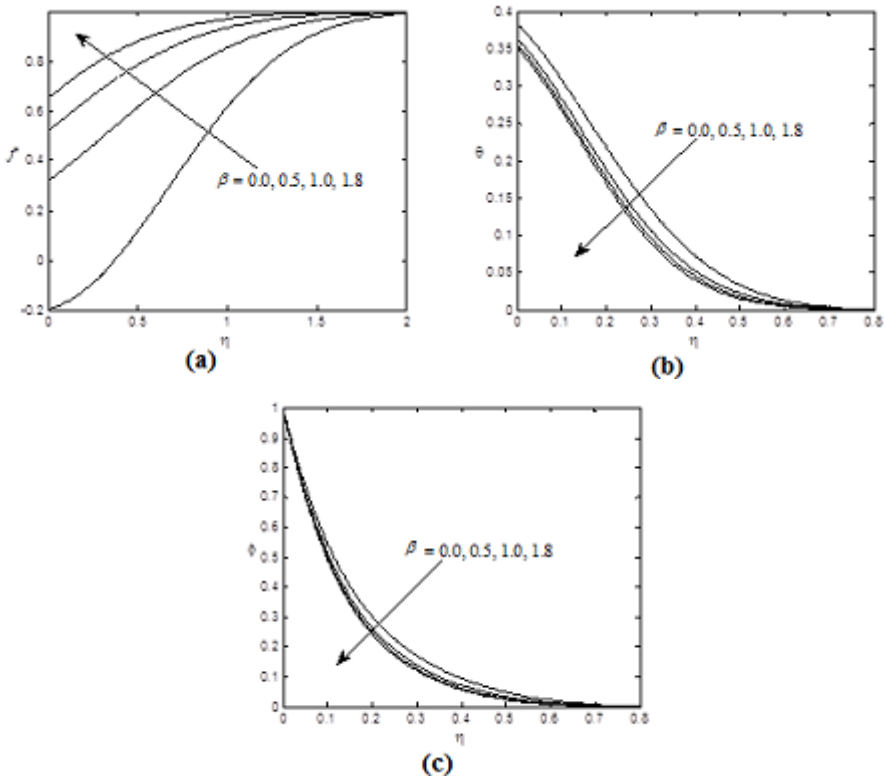

Fig. 4. Variation of dimensionless (a) velocity, (b) temperature and (c) nanoparticle volume fraction profiles for several values of wedge angle parameter β.

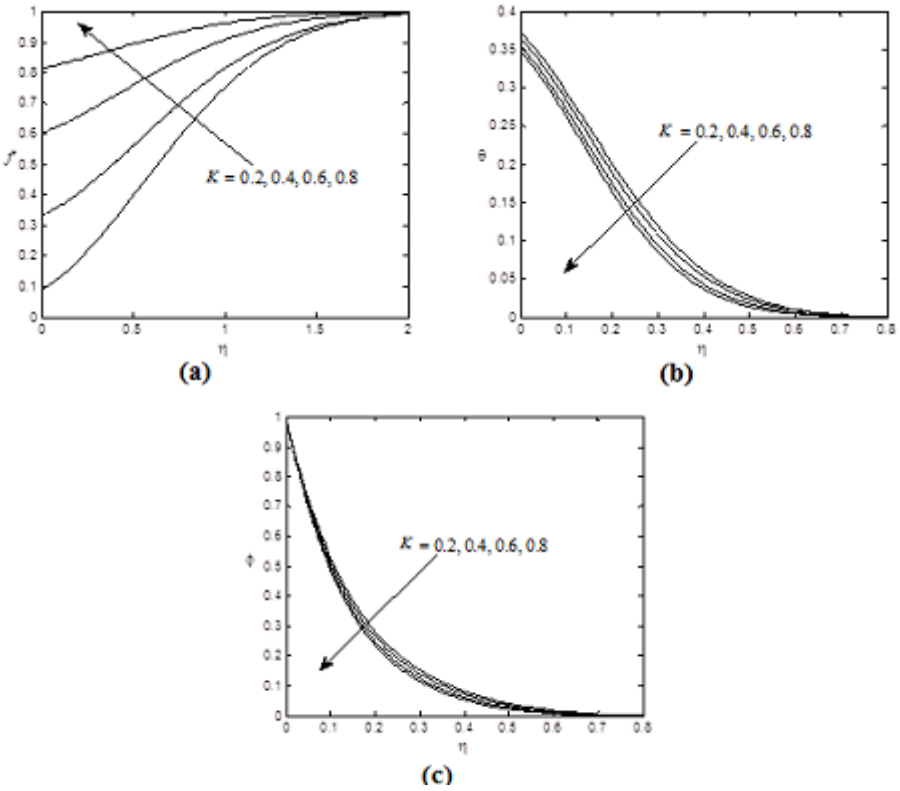

Fig. 5. Variation of dimensionless (a) velocity, (b) temperature and (c) nanoparticle volume fraction profiles for several values of unsteadiness parameter K.

within the boundary layer decreases with the increasing values of the wedge angle parameter β.

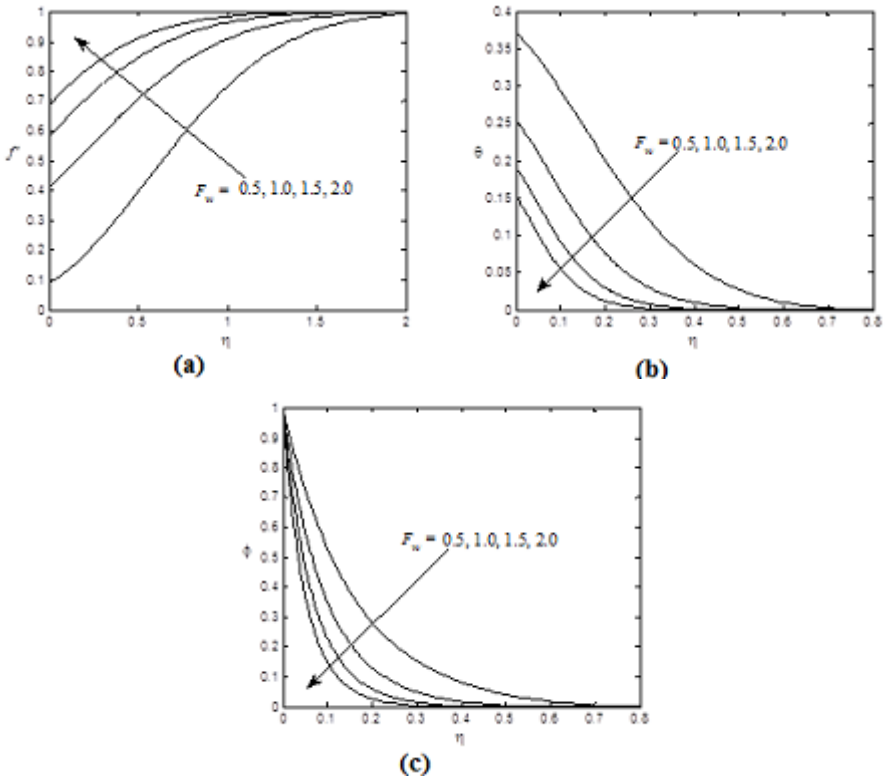

Fig. 6. Variation of dimensionless (a) velocity, (b) temperature and (c) nanoparticle volume fraction profiles for several values of suction parameter F_w.

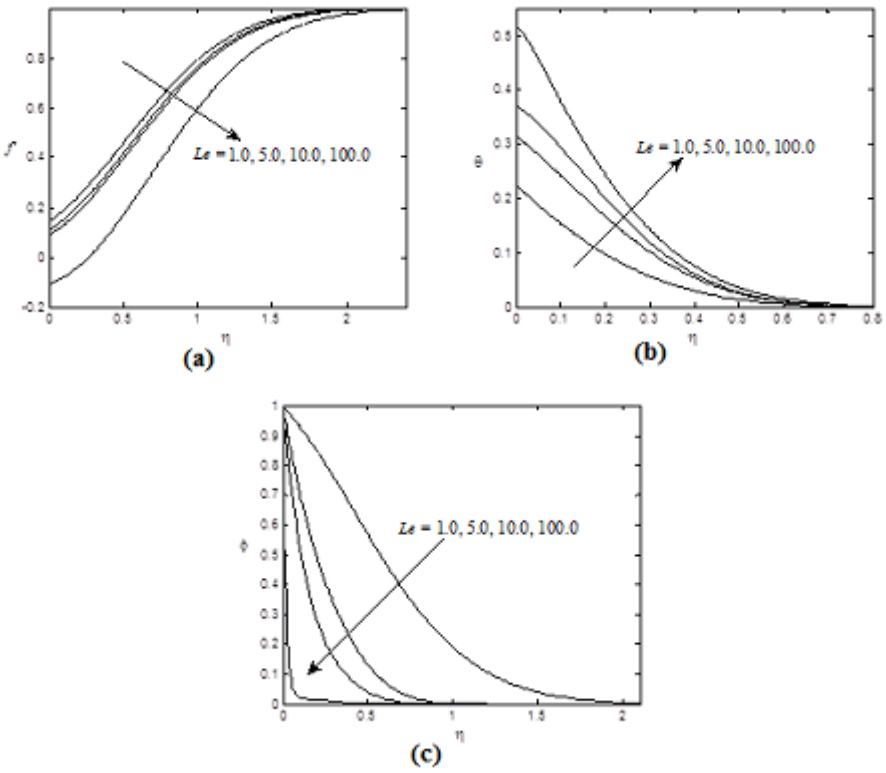

Fig. 7. Variation of dimensionless (a) velocity, (b) temperature and (c) nanoparticle volume fraction profiles for several values of Lewis number Le.

The effects of unsteadiness parameter K on the dimensionless velocity, temperature and nanoparticle volume fraction profiles within the boundary-layer have been displayed in Fig. 5(a)-(c) respectively. From these figures we

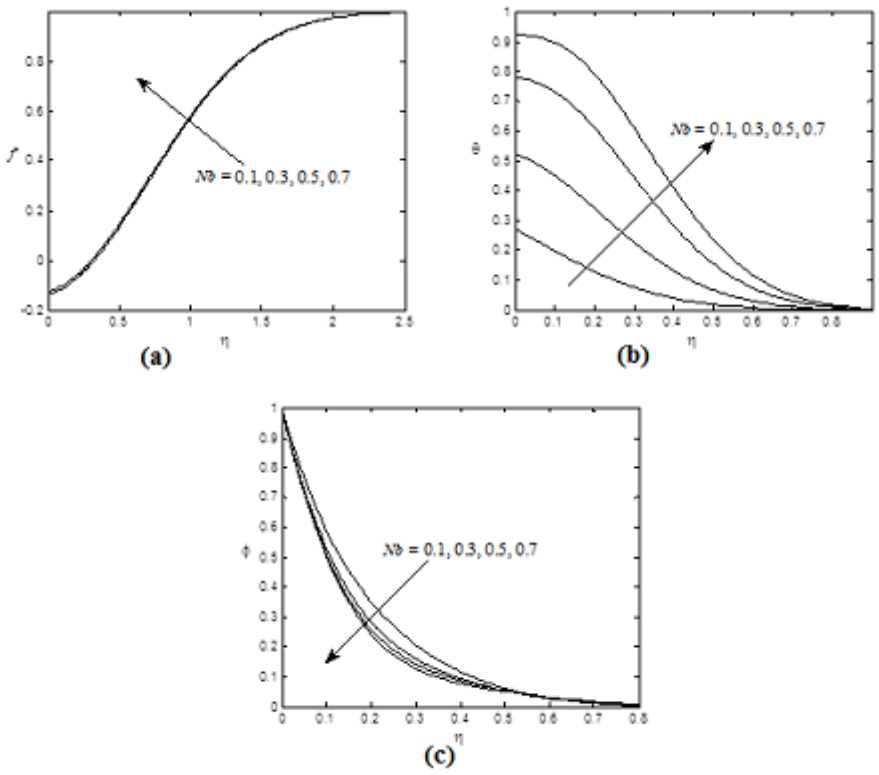

Fig. 8. Variation of dimensionless (a) velocity, (b) temperature and (c) nanoparticle volume fraction profiles for several values of Brownian motion parameter Nb.

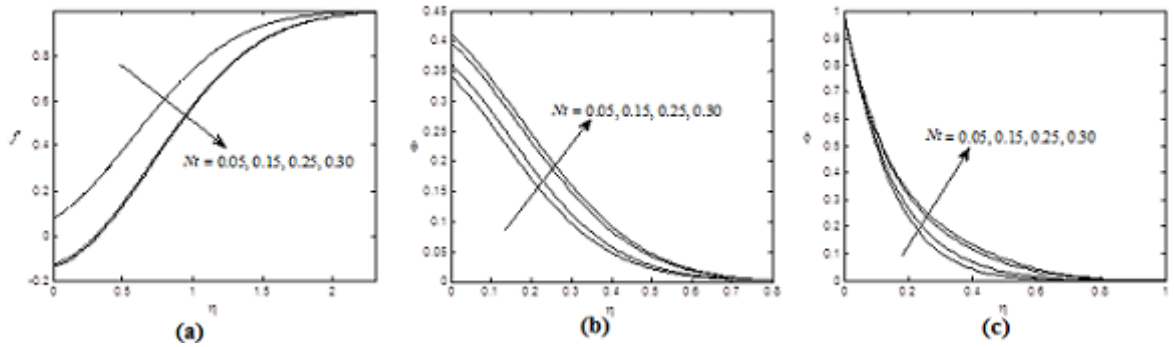

Fig. 9. Variation of dimensionless (a) velocity, (b) temperature and (c) nanoparticle volume fraction profiles for several values of thermophoresis parameter Nt.

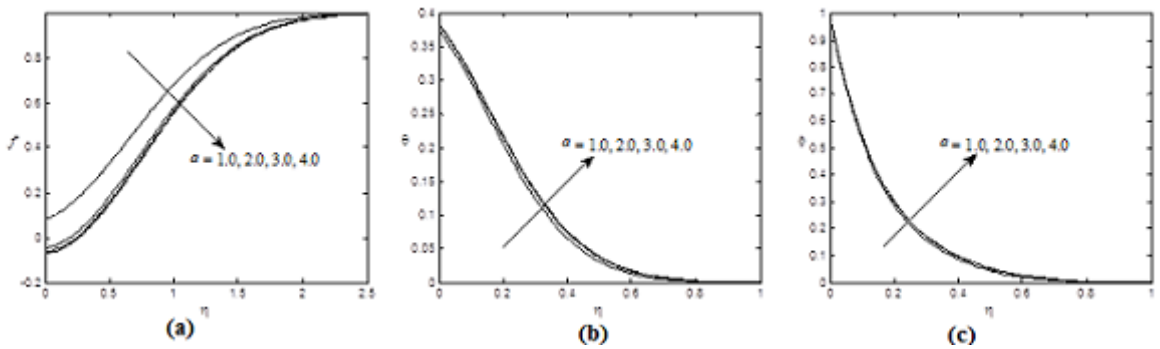

Fig. 10. Variation of dimensionless (a) velocity, (b) temperature and (c) nanoparticle volume fraction profiles for several values of first order slip parameter a.

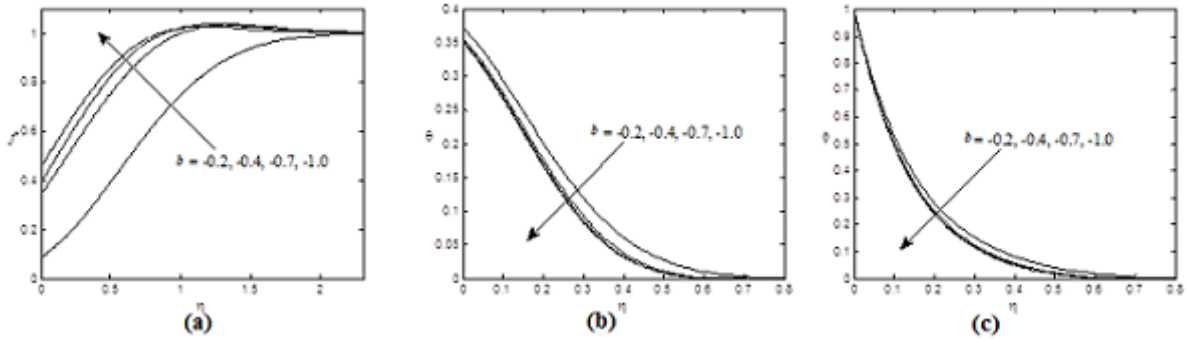

Fig. 11. Variation of dimensionless (a) velocity, (b) temperature and (c) nanoparticle volume fraction profiles for several values of second order slip parameter b.

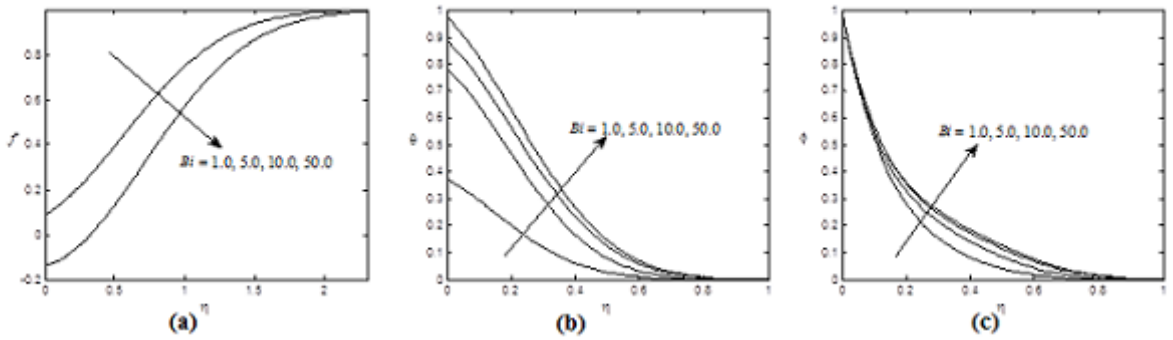

Fig. 12. Variation of dimensionless (a) velocity, (b) temperature and (c) nanoparticle volume fraction profiles for several values of Biot number Bi.

observe that velocity profiles within the boundary layer increases whereas both the temperature and nanoparticle volume fraction profiles decrease with the increasing values of the unsteadiness parameter K.

The effects of suction parameter F_w on the dimensionless velocity, temperature and nanoparticle volume fraction profiles within the boundary layer are shown in Fig. 6(a)-(c) respectively. From Fig. 6(a) we see that the fluid velocity within the boundary layer increases with the increase of the suction parameter F_w. It is also noticeable that the thickness of the hydrodynamic boundary layer decreases with the increase of the suction parameter. The physical explanation for such a behavior is that removal of the decelerated fluid particles through the porous surface reduce the growth of the boundary layer. Variation of both the temperature and the nanoparticle volume fraction profiles against η for different values of the suction parameter F_w are shown in Fig. 6(b)-(c) respectively. It is found that both the temperature and nanoparticle volume fraction within the boundary layer decrease with the increasing values of suction parameter. Suction therefore acts as a powerful mechanism for cooling of the device and such features are important in high temperature energy systems such as magnetohydrodynamic power generators, nuclear energy processes etc.

The effects of the Lewis number (Le) on the dimensionless velocity profiles within the boundary layer is shown in Fig. 7(a). From this figure we observe that the velocity profiles decreases with the increasing values of the Lewis number (Le). Fig. 7 (b) depicts the variation of the temperature profiles against for different values of the Lewis number. It is found that the temperature of the fluid within the boundary layer increases with the increasing values of the Lewis number . The effects of Lewis number on the nanoparticle volume fraction have been shown in Fig. 7(c). From this figure we see that there is a fall in the nanoparticle volume fraction with the increasing values of the Lewis number.

The effects of the Brownian motion parameter (Nb) on the dimensionless velocity profiles within the boundary layer is shown in Fig. 8(a). From this figure we observe that there is very small effect on the velocity profiles with the increasing values of the Brownian motion parameter (Nb). Volume fraction of nanoparticles is a key parameter for studying the effect of nanoparticles on the flow fields and temperature distributions. Thus Fig. 8(b) and Fig. 8(c) are prepared to present the effect of Brownian motion on temperature distribution and volume fraction of nanoparticles. From these figures we observe that the temperature of the fluid increases whereas the nanoparticles volume fraction decreases with the increasing values of the Brownian motion parameter (Nb). It is interesting to note that Brownian motion of the nanoparticles at the molecular and nanoscale levels is a key nanoscale mechanism governing their thermal behavior. In nanofluid system, due to the size of the nanoparticles, Brownian motion takes place which can affect the heat transfer properties. As the particle size scale approaches to the nano-meter scale, the particle Brownian motion and its effects on the surrounding liquids play an important role in heat transfer.

The effects of the thermophoresis parameter (Nt) on the dimensionless velocity profiles within the boundary layer is shown in Fig. 9(a). From this figure we observe that the velocity profiles decreases with the increasing values of the thermophoresis parameter (Nt). Fig. 9(b)-(c) respectively depict the variation of the temperature and nanoparticle volume fraction profiles against η for different values of the thermophoresis parameter (Nt) . From these figures it is clearly seen that both the temperature of the fluid and nanoparticle volume fraction profiles within the boundary layer increase with the increasing values of the thermophoresis parameter (Nt) and hence the nanoparticles enhance heat and mass transfer.

The effects of the first order slip parameter (a) on the dimensionless velocity, temperature and nanoparticle volume fraction profiles within the boundary layer is shown in Fig. 10(a)-(c) respectively. From Fig. 10(a) we observe that the velocity profiles decrease with the increasing values of first order slip parameter (a). Fig. 10(b)-(c) respectively depict the variation of the temperature and nanoparticles volume fraction profiles against η for different values of the first order slip parameter (a). From these figures it is clearly seen that both the temperature of the fluid and nanoparticle volume fraction profiles within the boundary layer increase with the increasing values of the first order slip parameter (a).

Fig. 11(a)-(c) respectively show the non-dimensional velocity, temperature and nanoparticle volume fraction profiles within the boundary layer for different values of the second order slip parameter (b). The behavior of these figures are just opposite to the Fig. 10(a)-(c) respectively. This behavior is consistent with the works of Rahman et al. [19]. Thus, the first and second order slips play an important role in modeling boundary layer flows with nanofluids over a stretching/shrinking surface.

The effects of Biot number (Bi) on the dimensionless velocity, temperature and nanoparticle volume fraction profiles within the boundary layer is shown in Fig. 12(a)-(c) respectively. From Fig. 12(a), we observe that the velocity profiles decrease with the increasing values of Biot number. The effects of the Biot number (Bi) on the temperature profiles against η are displayed in the Fig. 12(b). From this figure we observe that the temperature profiles within the boundary layer increase with the increase of the Biot number (Bi) which is consistent with the work of Rahman and Sattar [23]. The surface convection parameter or Biot number is a ratio of the hot fluid side convection resistance to the cold fluid side convection resistance on a surface. For fixed cold fluid properties and fixed free stream velocity, the surface convection parameter (Bi) at any station is directly proportional to the heat transfer coefficient, h_f associated with the hot fluid. The thermal resistance on the hot fluid side is inversely proportional to h_f. As Bi increases, the hot fluid side convection resistance decreases and consequently, the surface temperature increases. From this figure it is also confirmed that for large values of Bi i.e. $Bi \to \infty$, the temperature profile attains its maximum value 1.Thus the convective boundary condition become the prescribed surface temperature case. From Fig. 12(c) we observe that the nanoparticle volume fraction profiles within the boundary layer increase with the increasing values of the Biot number (Bi).

Table 2. Numerical values of $f''(0)$, $-\theta'(0)$ and $-\phi'(0)$ for different values of a, b and Bi.

a	b	Bi	$f''(0)$	$-\theta'(0)$	$-\phi'(0)$
1.0	-0.2	1.0	0.190586586237427	0.623620461742228	6.19574747453739
2.0	-0.2	1.0	0.0632770890398914	0.61679484137168	6.04675805959774
3.0	-0.2	1.0	0.0397395279321244	0.615836284090412	6.02617961203087
4.0	-0.2	1.0	0.0290440215297228	0.615420872374614	6.01728629223127
5.0	-0.2	1.0	0.022900826181098	0.61518754373066	6.01229756775012
0.5	-0.1	1.0	0.24728640840377	0.628887280285359	6.11388563814273
0.5	-0.2	1.0	0.350809002513481	0.626176857946244	6.23841283568729
0.5	-0.5	1.0	0.844458439970318	0.636281917841971	6.37924956653864
0.5	-0.7	1.0	0.911429132997759	0.647163014115693	6.66166907677987
0.5	-1.0	1.0	0.928705450584269	0.649216215490463	6.71559448104424
0.5	-0.2	0.5	0.350809002513501	0.391795158905951	6.32426800161239
0.5	-0.2	1.0	0.350809002513481	0.626176857946244	6.23841283568729
0.5	-0.2	5.0	0.350809000149636	1.08021250309119	6.14809289095227
0.5	-0.2	10.0	0.12697449662475	1.11692362179543	5.86740755210987
0.5	-0.2	50.0	0.12697449662475	1.17979749473617	5.86981318916675

Finally, the effects of the first and second order slip parameters as well as Biot number (or surface convection parameter) on the local skin friction coefficient, the local Nusselt number and the local Sherwood number are shown in Table 2. From Table 2, we see that the local skin friction coefficient, the local Nusselt number and the local Sherwood number decrease with the increasing values of the first order slip parameter a. On the other hand, from Table 2, we see that the local skin friction coefficient, the local Nusselt number and the local Sherwood number increase with the

increasing values of the second order parameter b. From this table we also see that the local skin friction coefficient and the local Sherwood number decrease whereas the local Nusselt number increase with the increasing values of the Biot number (Bi).

9. Conclusions

In this paper, we have developed a mathematical model of unsteady forced convective heat and mass transfer flow of nanofluid along a porous wedge with variable suction and second order slip. The model used for the nanofluid incorporates the effects of Brownian motion and thermophoresis. The potential flow velocity has been taken as a function of the distance x and time t. Fluid suction is imposed on the wedge surface. The governing time dependent non-linear partial differential equations are reduced to a set of non-linear ordinary differential equations by introducing an appropriate similarity transformations. The resulting local similarity equations for unsteady flow have been solved numerically by applying the function bvp4c from MATLAB for different values of the parameters. Since no experimental results of the corresponding studies are available, the obtained numerical results have been compared with that of the established numerical results which shows excellent agreement. The numerical results for the dimensionless parameters are presented in graphically and also in tabular form and analyzed them from the physical point of view. Based on the numerical results, the following important conclusions are summarized:

- Base fluids and nanoparticles play an important role in heat transfer.
- Addition of nanoparticles to the base fluid may not always increase the rate of heat transfer. It significantly depends on the surface convection and type of base fluid.
- Suction stabilizes the growth of the boundary layer.
- Velocity profiles within the boundary layer increase with the increase of the wedge angle parameter, unsteadiness parameter, shrinking parameter and second order slip parameter whereas it decrease with the increase values of the stretching parameter, Lewis number, thermophoresis parameter and first order slip parameter.
- Temperature within the boundary layer decreases with the increase of the wedge angle parameter, unsteadiness parameter and second order slip parameter while it increases with the increasing values of the Lewis number, Brownian motion parameter, thermophoresis parameter, first order slip parameter and Biot number (or surface convection parameter).
- Nanoparticle volume fraction within the boundary layer decreases with the increasing values of the wedge angle parameter, unsteadiness parameter, Lewis number ,Brownian motion parameter and second order slip parameter while it increases with the increasing values of the thermophoresis parameter, first order slip parameter and Biot number (or surface convection parameter).
- The local skin friction coefficient increases with the increase values of the second order slip parameter whereas it decrease with the increasing values of first order slip parameter as well as Biot number (or surface convection parameter).
- The local Nusselt number increases with the increasing values of the second order slip parameter and Biot number while it decreases with an increasing values of the first order slip parameter.
- The local Sherwood number increases with the increasing values of the second order slip parameter while it decreases with the increasing values of the first order slip parameter and Biot number.

References

[1] S.U.S. Choi, Enhancing thermal conductivity of fluids with nanoparticle. in: D. A. Siginer, H.P. Wang (Eds.), Developments and Applications of Non-Newtonian Flows, ASME FED, 231/MD 66 (1995) 99-105.
[2] H. Masuda, A. Ebata, K. Teramae, N. Hishinuma, Alteration of thermal conductivity and viscosity of liquid by dispersing ultra-fine particles. Netsu Bussei 7 (1993) 227-233.
[3] J. Buongiorno, W. Hu, Nanofluid coolants for advanced nuclear power plants, Paper no. 5705, in: Proceedings of ICAPP '05, Seoul, May 15-19, 2005.
[4] H. F. Oztop, E. Abu-Nada, Numerical study of natural convection in partially heated rectangular enclosures filled with nanofluids, Int. J. Heat Fluid Flow 29 (2008) 1326-1336.
[5] S.U.S. Choi, Z.G. Zhang, W. Yu, F.E. Lockwood, E.A. Grulke, Anomalously thermal conductivity enhancement in nanotube suspension. Appl. Phys. Lett. 79 (2001) 2252-2254.
[6] S. Kakac, A. Pramuanjaroenkij, Review of convective heat transfer enhancement with nanofluids, Int. J. Heat Mass Transfer 52 (2009) 3187-3196.

[7] S. K. Das, S.U.S. Choi, W. Yu, T. Pradeep, Nanofluids: Science and Technology. Wiley Interscience, New Jersey, 2007.
[8] J. Buongiorno, Convective transport in nanofluids. ASME J. Heat Transfer 128 (2006) 240-250.
[9] N. Bachok, A. Ishak, I. Pop, Boundary layer flow of nanofluids over a moving surface in a flowing fluid, Int. J. Thermal Sciences 49 (2010) 1663-1668.
[10] W. A. Khan, I. Pop, Boundary layer flow past a wedge moving in a nanofluid, Mathematical Problems in Engineering, Article ID 637285 (2013) 1-7.
[11] G. R. Rajput, J. S. V. R. Krishnaprasad, M. G. Timol, Application of scaling group transformation for MHD boundary layer flow and heat transfer of nanofluids over moving surface subject to suction/injection in the presence of thermal radiation with chemical reaction, Int. J. Adv. Appl. Math. Mech. 3(1) (2015) 139-144.
[12] M. A. Sattar, A local simialrity transformation for the unsteady two-dimensional hydrodynamic boundary layer equations of a flow past a wedge, Int. J. appl. Math. and Mech. 7 (2011) 15-28.
[13] T. Fang, S. Yao, J. Zhang, A. Aziz, Viscous flow over a shrinking sheet with a second order slip flow model, Commun. Nonliear Sci. Numer. Simul. 15 (2010) 1831-1842.
[14] M. S. Alam, M. N. Huda, A new approach for local similarity solutions of an unsteady hydromagnetic free convective heat transfer flow along a permeable flat surface, Int. J. Adv. Appl. Math. Mech. 1(2) (2013) 39-52.
[15] M. S. Alam, M. M. Haque, M. J. Uddin, Unsteady MHD free convective heat transfer flow along a vertical porous flat plate with internal heat generation, Int. J. Adv. Appl. Math. Mech. 2(2) (2014) 52-61.
[16] ATM. M. Rahman, M. S. Alam, M. K. Chowdhury, Local similarity solutions for unsteady two- dimensional forced convective heat and mass transfer flow along a wedge with thermophoresis, Int. J. Applied Mathematics and Mechanics 8(8) (2012) 86-112.
[17] M. M. Rahman, M.A. Al-Lawatia, I.A. Eltayeb, N. Al-Salti, Hydromagnetic slip flow of water based nanofluids past a wedge with convective surface in the presence of heat generation (or) absorption, Int. J. Therm. Sci. 57 (2012)172-182.
[18] M. M. Rahman, I.A. Eltayeb, Radiative heat transfer in a hydromagnetic nanofluid past a non-linear stretching surface with convective boundary condition, Meccanica 48 (2013) 601-615.
[19] M. M. Rahman, A. V. Rosca, I. Pop, Boundary layer flow of a nanofluid past a permeable exponentially shrinking/stretching surface with second order slip using Buongiorno's model, Int. J. Heat and Mass Transfer 77 (2014) 1133-1143.
[20] L. F. Shampine, I. Gladwell, S. Thompson, Solving ODEs with MATLAB, Cambridge University Press, 2003.
[21] L. F. Shampine, M.W. Reichelt, J. Kierzenka, Solving boundary value problems for ordinary differential equations in Matlab with bvp4c, 2010. http:// www.mathworks.com/bvp_tutorial
[22] F. M. White, Viscous Fluid Flows, Third ed. McGraw-Hill, New York, 2006.
[23] M. M. Rahman, M. A. Sattar, Nonlinear forced convective hydromagnetic flow of unsteady biomagnetic fluid over a wedge with convective surface condition, Chaos, Complexity and Leadership 49 (2012) 423-452.